

# Method to Generate Artificial Earthquake Accelerations with Time Domain Enhancement and Attenuation Characteristics

He Zhang<sup>1</sup>, Marius Bittner<sup>2</sup>, Michael Beer<sup>2</sup>

<sup>1</sup> College of Civil Science and Engineering, Yangzhou University, Yangzhou 225127, China

<sup>2</sup> Institute for Risk and Reliability, Leibniz University Hannover, Hannover 30167, Germany

\*Correspondence should be addressed to He Zhang; scottz14@126.com

**Abstract:** To generate artificial earthquake acceleration time histories that perform the same enhancement and attenuation characteristics as natural ones, 500 natural earthquakes have been statistically analyzed. And these natural earthquakes have been divided into 5 groups by D5-95 durations. Each edge envelope curve which is used as the standard time history envelope curve for each D5-95 earthquake group has been proposed, and the ratio of earthquake samples that are covered by the edge envelope to the group total is described by the coverage rate. Under the 75% coverage rate, edge envelope curves of different D5-95 groups were fitted as exponential envelope function and compound envelope function, and parameters were solved. In each D5-95 group, 1200 artificial earthquakes' acceleration time histories with different intensities were generated according to the Chinese standard response spectrums and multiplied with these two envelope functions. Comparing maximum values of initial earthquakes' mean spectrum and that of enveloped earthquakes' mean spectrum, amplitude adjustment coefficients were given to maintain earthquakes' intensity. And after adjusted, the results of the goodness of fitting regression analysis shown artificial earthquakes' mean spectrums are 90% explaining accuracy to initial earthquakes' mean spectrums.

**Keywords:** Artificial Time History, Earthquake Ground Acceleration, Time-Domain Peak Reduction

## Introduction

Structural seismic analysis can be treated as a process that inputting signals to the calculation system and output results [1]. The inputting signals are earthquake time histories, and the most widely used are ground acceleration time histories, and output results are structural responses [2]. The most interesting structural response in seismic designing is the deformation response, and deformation based designed has been introduced in the seismic designing code of the US, EU, and China. For instance, there are three basic requirements for structural responses in Chinese standard "Code for Seismic Design for Buildings" GB50011-2010 [3] are:

(1) the structure should be no damage state and can continue safety living without to be repaired after suffering a frequent earthquake;

(2) the structure should be limited damage state and can continue safety living by a general repairment after suffering a seismic precautionary intensity earthquake;

(3) the structure should not collapse after suffering a rare earthquake.

And all these requirements have their deformation limiting values for failure.

Normally, one building project can be designed to be multiple structure designing schemes that match these all 3 requirements of GB50011. For choosing the best scheme for the designing, it is necessary to compare the pros and cons of these scheme by a characteristic which can reflect safety in structural service life for seismic. Seismic failure risk is defined by failure probabilities when a structure suffers a large number of earthquakes, and it is a characteristic to describe the reliability of structural seismic safety quantitatively.

Reliability in structural engineering means the structure can safe performance when suffering expected acts in the expected service time (GB50068 2018)[4]. In China, for structural seismic reliability analysis, the expected act means random ground motions which GB50011 prescribed appearance probability, and the expected service time for most buildings is 50 years.

Monte Carlo Simulation method is efficient for reliable analysis [5]. It is a method that inputting multiple signals with different random values of specific variables that obey a scheduled distribution to systems, then statistical analyzing outputs. In seismic reliability analysis, random signals are earthquake time histories. And intensity is the most important variable to reflect serious earthquakes' destruction, it can be described by ground motion parameters. Relates between intensity and ground motion parameters are shown in Table 1(GB/T17742 2008) [6]. And according to GB50011, the relation between intensity and extreme value of seismic influence coefficient  $\alpha_{s0}$  which is the peak value of the standard response spectrum is shown in Table 2, where  $g$  is the gravitational acceleration. And probability distribution of each intensity's earthquake appears is extreme value distribution.

For structural seismic risk evaluation by the Monte Carlo Simulation method, large numbers of earthquake data are required. The most direct method is using actual records of natural earthquakes. However, in most cases, using time histories from actual earthquake data has many limitations for many reasons [7]. And the most difficult is that there are not enough actual records of different seismic intensities in many regions for structural seismic risk analysis. Thus, structural reliable analysis needs to

generate artificial earthquake signals based on random intensities.

**Table 1** Earthquake parameters corresponding to intensities in GB/T17742-2008

Intensity	peak ground acceleration $\text{m} \cdot \text{s}^{-2}$	peak ground velocity $\text{m} \cdot \text{s}^{-1}$
5	0.22~0.44	0.02~0.04
6	0.45~0.89	0.05~0.09
7	0.90~1.77	0.10~0.18
8	1.78~3.53	0.19~0.35
9	3.54~7.07	0.36~0.71
10	7.08~14.14	0.72~1.41

**Table 2** Extreme values of seismic influence coefficient  $a_{s0}$

Intensity	$a_{s0}(g)$
5	0.02~0.04
6	0.05~0.09
7	0.10~0.18
8	0.19~0.35
9	0.36~0.71
10	0.72~1.41

To make artificial earthquakes have a similar feature as actual earthquakes in the frequency domain and time domain, intensities and enhancement-attenuation time process must obey the same rules. The response spectrum reflected the reactive degree of single degree freedom systems with different natural vibration periods when suffering an earthquake, and it has a functional relationship with the signal's Fourier spectrum. The standard response in designing code can reflect representative characteristics of earthquakes in regions, and it is defined by regional seismic precautionary intensity. Kost [8] proposed a relation function between earthquakes' response spectrums and their Fourier spectrums, thus artificial earthquakes based on given response spectrums can be generated by using the inverse Fourier process (IFFT), and this method is wild used.

But different from natural earthquakes which are contain enhanced stage and attenuation stage, initial artificial earthquakes that are generated by the Fourier process without adjusted and enveloped are constant amplitudes approximately. To propose earthquake time history envelopes functions which have adequate representation to natural earthquakes, 500 earthquakes have been statistically analyzed, and edge envelopes that are treated to be standard envelope curves and their representatives are valued by coverage rates have been defined in this paper. By using software MATLAB, edge envelopes have been fitted by two most common envelope equations. And a method that includes artificial ground acceleration generation, enveloping, and amplitude adjusting have been proposed, and it can generate random intensity signals based on a given standard response spectrum to be inputting data for structural reliable analysis by the Monte Carlo Simulation method.

### Random earthquake signal generation

The response spectrum is an envelope of peak earthquake response (displacement, velocity, and acceleration) from a series of single degree of freedom (SDOF) systems whose self-vibration periods ( $T$ ) are different. Mostly, it is expressed as acceleration spectrum  $S_a$ , and  $S_a$  can transfer to deformation spectrum  $S_d$  as it is shown in Eq.1.

$$S_d = \left(\frac{T}{2\pi}\right)^2 S_a \quad (1)$$

To SDOF system, according to D'Alembert's principle:

$$m\ddot{x} + c\dot{x} + kx = -m\ddot{x}_g \quad (2)$$

If ignore damping, and define:

$$F = -(m\ddot{x} + m\ddot{x}_g) \quad (3)$$

So that:

$$kx = F \quad (4)$$

According to Duhamel's integral,

$$k = m \cdot \omega^2 \quad (5)$$

$x$  is system displacement,  $k$  is system stiffnesses,  $c$  relates to system damping, and  $\omega = 2\pi/T$  is the angular frequency of the system.

$$x = -\frac{1}{\omega} \int_0^t \ddot{x}_g(\tau) e^{-\zeta\omega(t-\tau)} \sin\omega(t-\tau) d\tau \quad (6)$$

$$F = m\omega \left| \int_0^t \ddot{x}_g(\tau) e^{-\zeta\omega(t-\tau)} \sin\omega(t-\tau) d\tau \right|_{\max} \quad (7)$$

$\zeta$  is the damping factor, and define:

$$F = m \cdot S_a \quad (8)$$

$$S_a = \frac{2\pi}{T} \left| \int_0^t \ddot{x}_g(\tau) e^{-\zeta\omega(t-\tau)} \sin\omega(t-\tau) d\tau \right|_{\max} \quad (9)$$

According to Eq.8 and Eq.9, the inertia force  $F$  can be calculated if a ground acceleration time ( $t$ ) history  $\ddot{x}_g(t)$  is input into an SDOF system of which the damping factor is  $\zeta$ . And define the seismic influence coefficient  $a_s$ :

$$a_s = S_a / g \quad (10)$$

Standard response spectrums are given by different seismic design codes (GB50011, EC8[9], ASCE 7[10]), these standard spectrums are summary and simplified to earthquakes which have happened in this country or region, and it is easy to use on seismic design. And the standard response spectrum of Chinese code GB50010 is shown in Figure1. Where:

$$\gamma = 0.9 + \frac{0.05 - \zeta}{0.3 + 6\zeta} \quad (11)$$

$$\eta_1 = 0.02 + \frac{0.05 - \zeta}{4 + 32\zeta} \quad (12)$$

$$\eta_2 = 1 + \frac{0.05 - \zeta}{0.08 + 1.6\zeta} \quad (13)$$

$\zeta$  is the damping ratio.

A relationship function between  $S_a$  to earthquakes determines the power spectral density function (PSDF) had been proposed by Kaul, M. K.[11] as it is shown in Eq.14.

$$f(\omega) = \frac{2\zeta}{\pi\omega} \cdot S_a^2 / \left\{ -2\ln \left[ \frac{-\pi}{\omega t_{\max}} \ln(1-r) \right] \right\} \quad (14)$$

Where  $r$  is the value of the exceedance probability,  $t_{\max}$  is earthquake duration.

And artificial earthquake acceleration signal can be generated by Eq.15 to Eq.16 [12].

$$a_{cc}(t) = I(t) \sum A(\omega) \sin(\omega t + \varphi_r) \quad (15)$$

$$A = \sqrt{4f(\omega) \Delta\omega} \quad (16)$$

Where  $a_{cc}$  if acceleration time histories,  $I(t)$  is envelope function of acceleration time history,  $\varphi_r$  is

rand number which changes from  $-2\pi$  to  $2\pi$ ,  $\Delta\omega$  is the increment gradient value of  $\omega$  in each step.

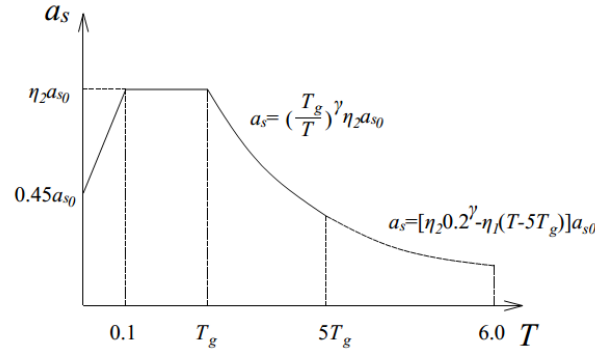


**Figure 1.** Standard response spectrum of Chinese code GB50010

## Natural earthquakes' amplitudes-time laws and edge envelopes

### *Standard envelope curve functions and natural earthquake data*

The envelope curve of the earthquake means the connect curve of extreme points of earthquake time histories, and it is a describing of the earthquake's amplitudes-time changing law. Thus there are two envelope curves for one earthquakes signal (in the positive direction and the negative direction respectively), and by using extreme points connect curve of earthquakes absolutely values to simplify these two envelopes to one. As it is shown in Figure2, normalized time histories  $a_{cc}$  by its maximum value  $a_{max}$  to be  $|a_{cc}/a_{max}|$  of an artificial earthquake and a natural earthquake, and their intensities are constant values respectively, it can be observed that amplitudes of the artificial signal are nearly time unchanged, but amplitudes of the nature earthquake have a visible enhanced stage and attenuate stage with time  $t$  changes.

To imitate amplitudes-time changing laws of natural earthquakes, numerous earthquake envelope functions have been proposed, and the most widely used is the exponential envelope curve [13] and the compound envelope curve [14], their curve is shown in Figure3, and calculation equations are Eq.17 and Eq.18 respectively.

$$I(t) = A(e^{-\alpha t} - e^{-\beta t}) \quad (17)$$

$$I(t) = t/(b_1 t_{max}), \quad t/t_{max} \leq b_1$$

$$I(t) = 1, \quad b_2 \leq t/t_{max} \leq b_2 \quad (18)$$

$$I(t) = e^{(-\gamma(t/t_{max} - b_2))}, \quad t/t_{max} > b_2$$

To give function parameters of these two curves and make them fully representative of natural earthquakes, regression fitting by actual earthquake data to these two curve functions has been done in

the software Matlab. Fitting data is based on 500 earthquakes that are downloaded from the PEER (Pacific Earthquake Engineering Research Center) Strong Ground Motion Databases. And to distinguish amplitude changing characteristics of different time durations, these actual earthquakes are divided into 5 groups according to their D5-95 significant durations [16], as it is shown in Table 3.

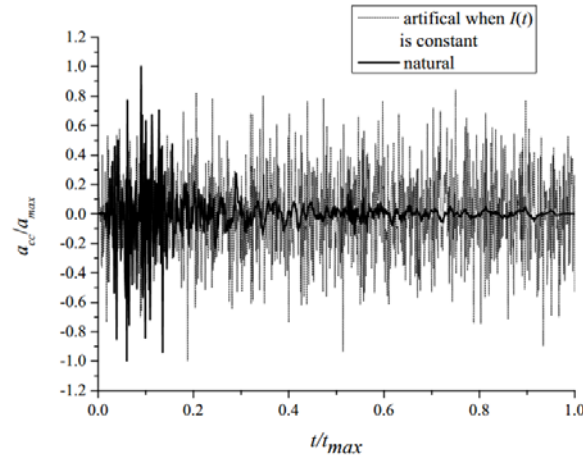


**Figure 2.** Relative exterior of artificial earthquake when  $I(t)$  is constant and one natural earthquake

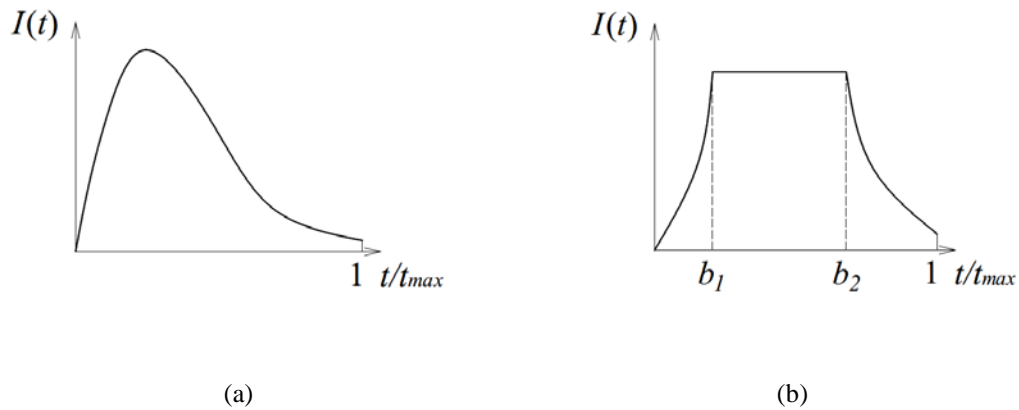


**Figure 3.** Earthquake envelope curves: (a) Exponential envelope; (b) Compound envelope

To give each standard curve which is not affected by duration for each D5-95 group, time  $t$  is normalized to be  $t/t_{max}$ , and acceleration  $a$  is normalized to be  $a/a_{max}$  of each earthquake. Extreme value points (tips, local maximum, and local maximum) of  $|a/a_{max}|$  have been connected to be envelope curves in the absolute value normalized coordinate system as it is shown in Figure4. And  $t/t_{max}$  values when an envelope's  $|a/a_{max}|$  increase to the value in Table 4 for the first time and decrease to these values at the last time have been marked out. Probability for  $F=P(t/t_{max} \leq x \mid |a/a_{max}|=y)$ ,  $x, y \in [0,1]$  of each earthquake

group is shown in Figure5.

**Table 3** D5-95 of significant durations of earthquake groups

Earthquake groups	D5-95 (s)
1	5 to 10
2	11 to 15
3	16 to 20
4	20 to 30
5	30 to 50

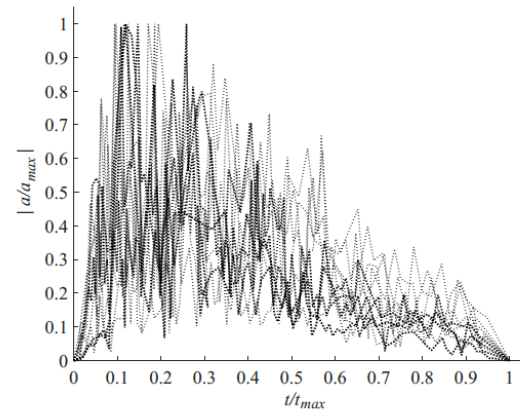
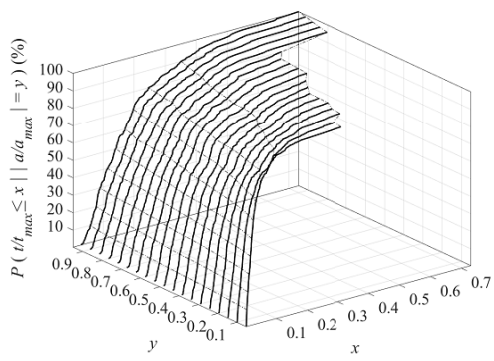
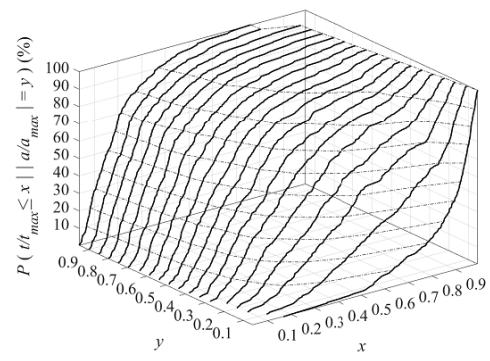


**Figure 4.** Envelope curve for each acceleration

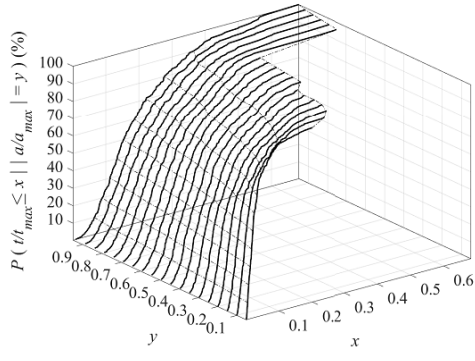


(a)

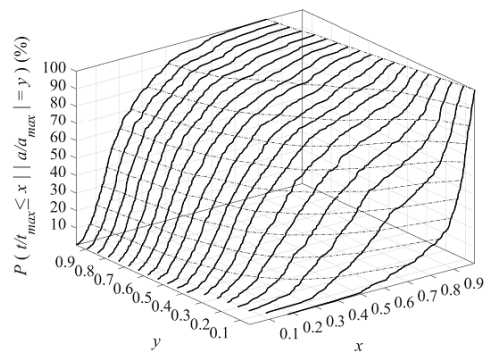


(b)

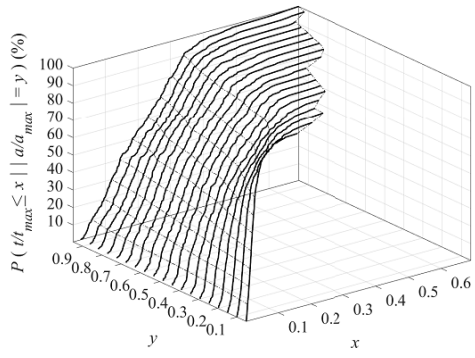




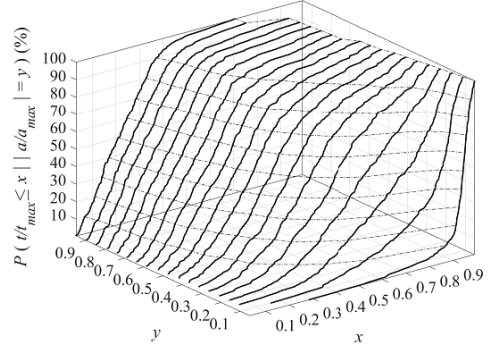
(c)



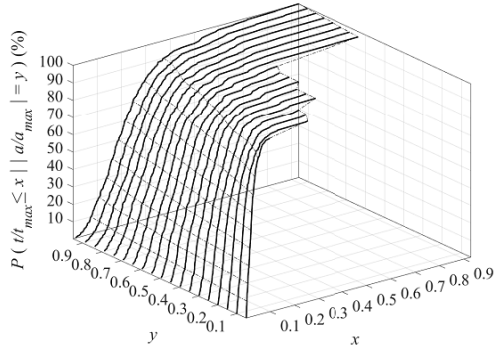
(d)



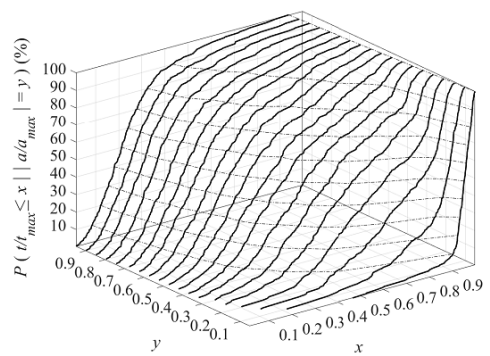
(e)



(f)



(g)



(h)

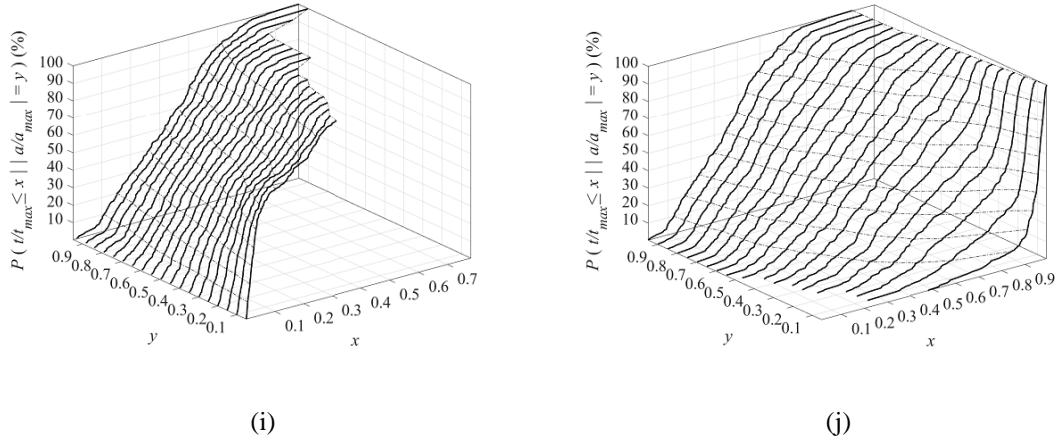


**Figure 5.**  $P(t/t_{max} \leq x | |a/a_{max}| = y)$ : (a) Group 1, enhancement stage; (b) Group 1, attenuation stage; (c) Group 2, enhancement stage; (d) Group 2, attenuation stage; (e) Group 3, enhancement stage; (f) Group 3, attenuation stage; (g) Group 4, enhancement stage; (h) Group 4, attenuation stage; (i) Group 5, enhancement stage; (j) Group 5, attenuation stage;

**Table 4** Statistics key points value ( $y$ )

Earthquake stages	$y$
Increasing stage	0.05 to 0.95, each step increases 0.95
Decreasing stage	0.95 to 0.05, each step decreases 0.95

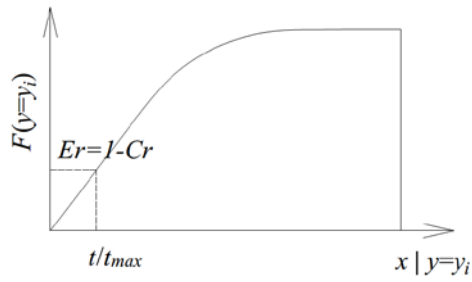
#### Edge envelop with the coverage rate

The coverage rate of an envelope for multiple earthquake signal sample  $Cr$  is defined as Eq.19.

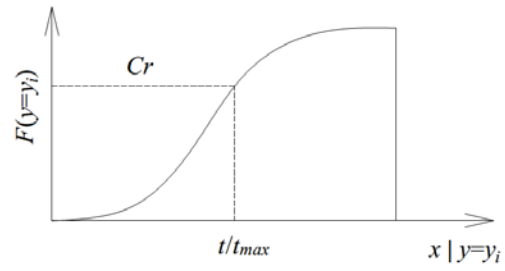
$$Cr = P(|a/a_{max}| \leq y | t/t_{max} = x) \quad (19)$$

And exceeding probability  $Er = 1 - Cr$ .  $Er$  and  $Cr$  is using for describing the representativeness of the artificial envelopes to earthquake samples that it is built basing on. E.g. if  $Er = 25\%$  ( $Cr = 75\%$ ) for an artificial envelope, points on the envelope should be  $t/t_{max} = x$  ( $F = 1 - Cr$ ) when the envelope is enhancement stage, and  $t/t_{max} = x$  ( $F = Cr$ ) when the envelope is attenuation stage. That means in the enhancement stage when  $|a/a_{max}| = y_i$ ,  $t/t_{max}$  in envelope curve is earlier than 75% ( $Cr$ ) earthquakes peak points data, and in the attenuation stage when  $|a/a_{max}| = y_i$ ,  $t/t_{max}$  in envelope curve is later than 75% ( $Cr$ ) earthquakes peak points data, thus 75% peak points of all earthquake samples are covered by the artificial envelope, as it is shown in Figure6, and this envelope called edge 'Cr=75% edge envelope'. Cr=75% edge envelopes of 5 different D5-95 earthquake groups are drawn in Figure7 and values of key points

are given in Table 5.

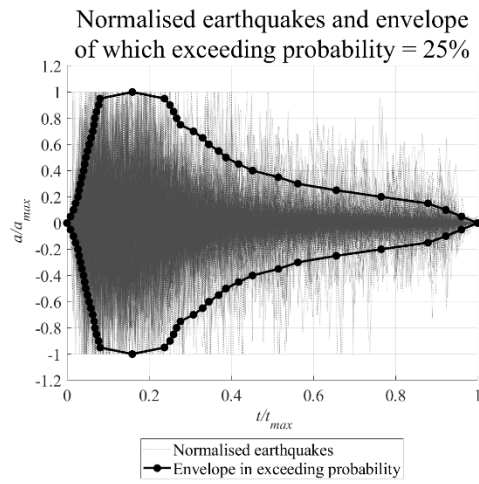


(a)

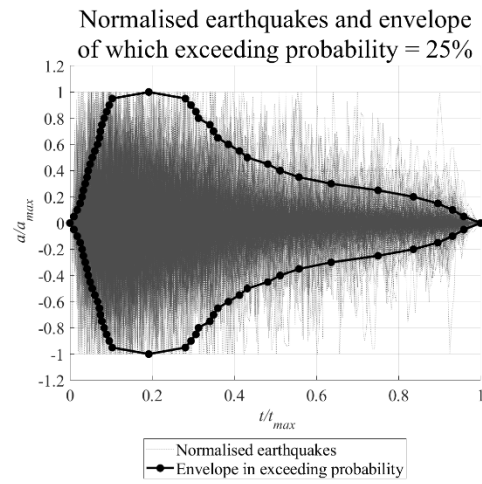


(b)

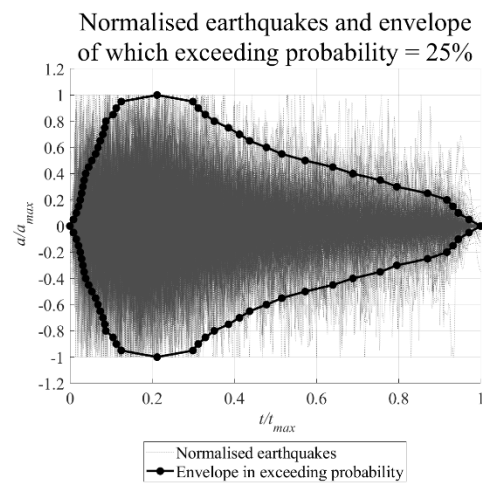
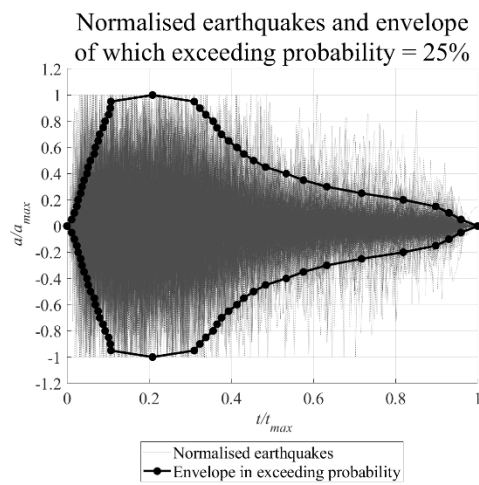
**Figure 6.** Assignment  $t/t_{max}$  values of the edge envelope curve by  $C_r$ : (a) enhancement stage; (b) attenuation stage

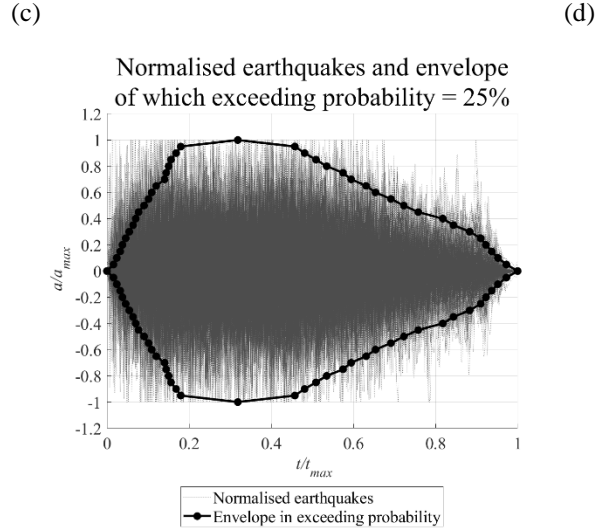


(a)



(b)





(e)

**Figure 7.**  $Cr=75\%$  ( $Er=25\%$ ) edge envelopes of 5 earthquake groups: (a) Group 1; (b) Group 2; (c) Group 3; (d) Group 4; (e) Group 5

**Table 5** Value of key points in edge envelope curves

$ a/a_{max} $	$t/t_{max}$				
	Group 1	Group 2	Group 3	Group 4	Group 5
0	0	0	0	0	0
0.05	0.009	0.010	0.011	0.009	0.016
0.1	0.016	0.018	0.018	0.016	0.024
0.15	0.021	0.025	0.024	0.021	0.032
0.2	0.027	0.030	0.027	0.025	0.038
0.25	0.030	0.033	0.034	0.028	0.046
0.3	0.033	0.037	0.037	0.032	0.054
0.35	0.036	0.042	0.042	0.034	0.064
0.4	0.041	0.045	0.049	0.038	0.070
0.45	0.043	0.049	0.052	0.046	0.077
0.5	0.046	0.054	0.057	0.053	0.091
0.55	0.050	0.061	0.067	0.063	0.102

**Continue-table 5** Value of key points in edge envelope curves

$ a/a_{max} $	$t/t_{max}$				
	Group 1	Group 2	Group 3	Group 4	Group 5
0.6	0.054	0.068	0.069	0.068	0.109
0.65	0.058	0.072	0.076	0.074	0.120
0.7	0.063	0.074	0.080	0.080	0.140
0.75	0.066	0.078	0.088	0.085	0.144
0.8	0.068	0.084	0.093	0.087	0.150
0.85	0.072	0.089	0.102	0.105	0.156
0.9	0.077	0.096	0.106	0.113	0.169
0.95	0.081	0.103	0.107	0.125	0.180
1	0.159	0.192	0.209	0.212	0.319
0.95	0.237	0.281	0.310	0.299	0.458
0.9	0.251	0.295	0.324	0.313	0.481
0.85	0.260	0.307	0.338	0.330	0.509
0.8	0.267	0.313	0.356	0.352	0.535
0.75	0.277	0.341	0.365	0.386	0.575
0.7	0.308	0.350	0.376	0.413	0.595
0.65	0.330	0.360	0.394	0.438	0.631
0.6	0.346	0.386	0.414	0.479	0.654
0.55	0.369	0.413	0.431	0.516	0.691
0.5	0.387	0.432	0.455	0.573	0.723
0.45	0.418	0.482	0.484	0.640	0.758
0.4	0.452	0.512	0.534	0.689	0.818
0.35	0.515	0.558	0.576	0.755	0.844
0.3	0.562	0.636	0.633	0.796	0.883
0.25	0.656	0.750	0.717	0.871	0.910

**Continue-table 5** Value of key points in edge envelope curves

$ a/a_{max} $	$t/t_{max}$				
	Group 1	Group 2	Group 3	Group 4	Group 5
0.2	0.765	0.836	0.819	0.918	0.923
0.15	0.879	0.896	0.898	0.933	0.937
0.1	0.922	0.931	0.930	0.946	0.952
0.05	0.961	0.959	0.959	0.972	0.973
0	1	1	1	1	1

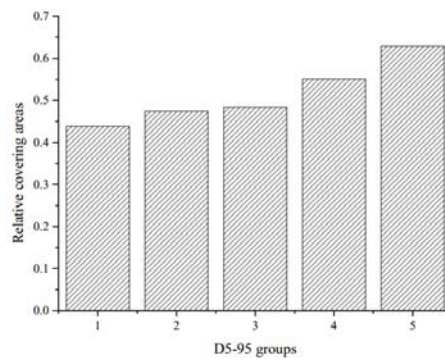
Based on values in Table 5, the relative time distance between points with same  $|a/a_{max}|$  value  $y_i$  in edge envelope curves have been calculated and shown in Table 6, the distance means  $t/t_{max(de)} - t/t_{max(in)}$ , of which  $t/t_{max(in)}$  is the relative time when  $|a/a_{max}| = y_i$  in the increase stage of the edge curve, and  $t/t_{max(de)}$  is the relative time when  $|a/a_{max}| = y_i$  in the decrease stage of the edge curve. Compared relative time distance of each relative amplitude  $|a/a_{max}|$  between each D5-95 groups, it can be observed that  $t/t_{max(de)} - t/t_{max(in)}$  of each relative amplitude increasing with the group's D5-95 duration increasing. It means a stronger amplitude of which  $|a/a_{max}|$  is higher value occupies more and more time-history proportion with D5-95 duration increasing. And compared relative covering areas (that are shown in Figure8) that are  $|a/a_{max}|$  integration respect to  $t/t_{max}$  of edge curves between D5-95 groups, it can be observed that the relative covering area increasing with group's D5-95 duration increasing. It reflects that based on current earthquakes samples, the longer D5-95 an earthquake is, the higher the energy density the earthquake contains.

**Table 6** Relative time distance between points with same  $|a/a_{max}|$  in edge envelope curves

$ a/a_{max} $	$t/t_{max(de)} - t/t_{max(in)}$				
	Group 1	Group 2	Group 3	Group 4	Group 5
0	1.000	1.000	1.000	1.000	1.000
0.05	0.952	0.949	0.948	0.963	0.957
0.1	0.907	0.914	0.912	0.930	0.928
0.15	0.858	0.871	0.874	0.912	0.904
0.2	0.738	0.807	0.792	0.892	0.885

**Continue-table 6** Relative time distance between points with same  $|a/a_{max}|$  in edge envelope curves

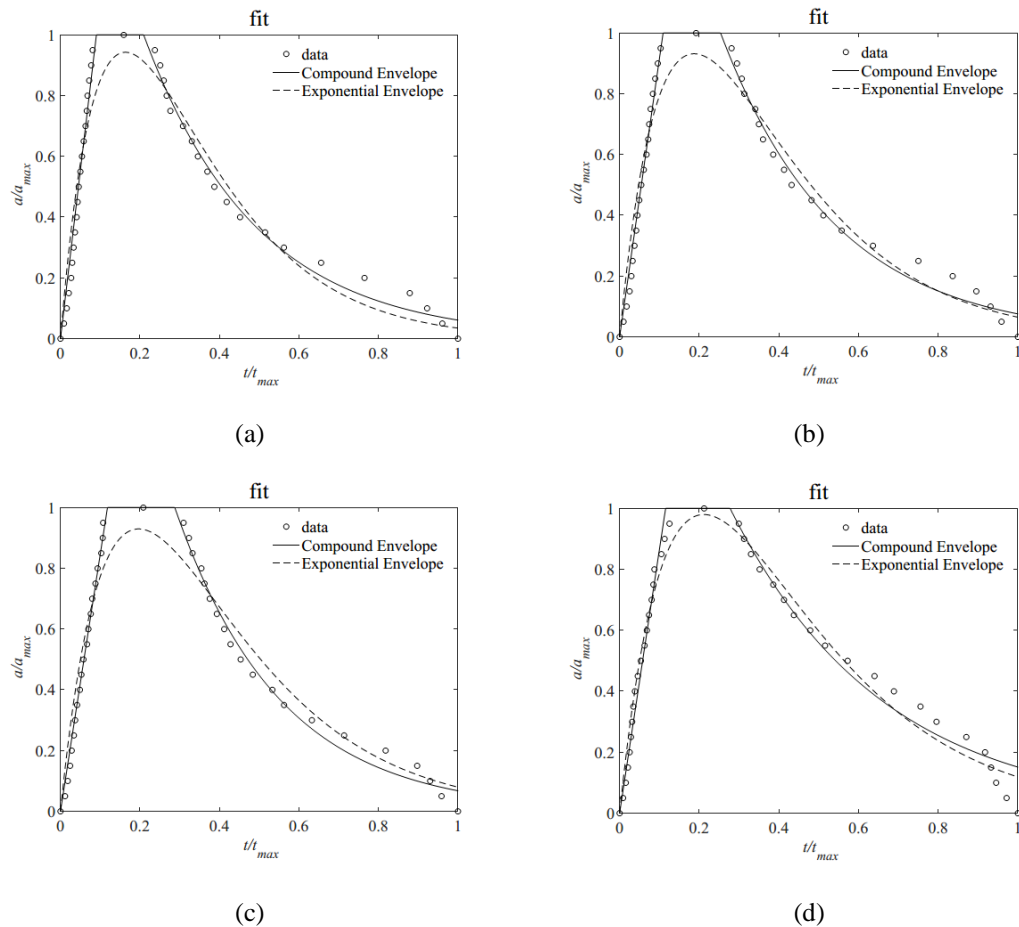
$ a/a_{max} $	$t/t_{max(de)} - t/t_{max(in)}$				
	Group 1	Group 2	Group 3	Group 4	Group 5
0.25	0.626	0.717	0.684	0.842	0.864
0.3	0.529	0.599	0.596	0.764	0.829
0.35	0.478	0.516	0.534	0.721	0.780
0.4	0.411	0.467	0.485	0.650	0.748
0.45	0.375	0.433	0.432	0.595	0.681
0.5	0.341	0.378	0.397	0.519	0.632
0.55	0.319	0.352	0.364	0.453	0.590
0.6	0.292	0.318	0.345	0.410	0.545
0.65	0.272	0.288	0.317	0.364	0.511
0.7	0.245	0.275	0.297	0.332	0.454
0.75	0.210	0.263	0.277	0.301	0.430
0.8	0.199	0.230	0.263	0.264	0.385
0.85	0.187	0.217	0.237	0.225	0.353
0.9	0.174	0.199	0.218	0.200	0.313
0.95	0.157	0.178	0.203	0.174	0.278
1	0.159	0.192	0.209	0.212	0.319



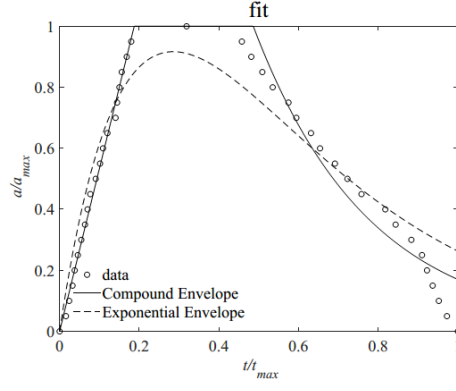
**Figure 8.** Relative covering areas of edge envelope curves

### Edge envelope curves fitting and error analysis

Edge curves of earthquake groups were fitted corresponding to Eq.17 and Eq.18 by using “Curve Fitting Tools” in software Matlab respectively. Fitted parameters are shown in Table 7 and Table 8, these fitted curves are shown in Figure9. Fitting residuals and coefficient of determination ( $r^2$ ) values of exponential envelopes and compound envelopes for each D5-95 group are shown in Figure10 respectively. And the coefficient of the determination  $r^2$  is a type measuring for quantifying the goodness-of-fit and its value is between 0 to 1 and as larger as better fitting [17]. It can be observed that all  $r^2$  values of these two type envelope functions are higher than 0.8 and it means 80% data of each D5-95 group's edge curve can be explained by its two type curve functions respectively, these functions are high goodness-of-fit. And  $r^2$  values of compound envelope curves' function fitting are higher than of exponential envelope curves' function fitting, and residuals of compound envelope curves' function fitting are smaller than that of exponential envelope curves' function fitting, thus the function type of the compound envelope is more accurate for edge envelope curves fitting than the exponential envelope's function type.

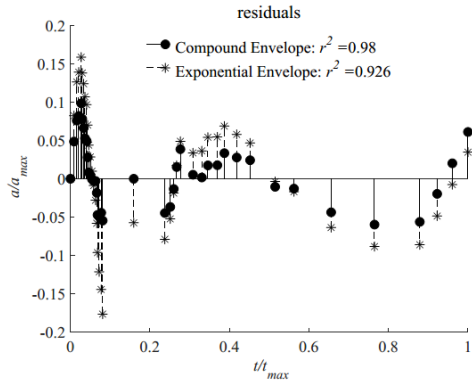




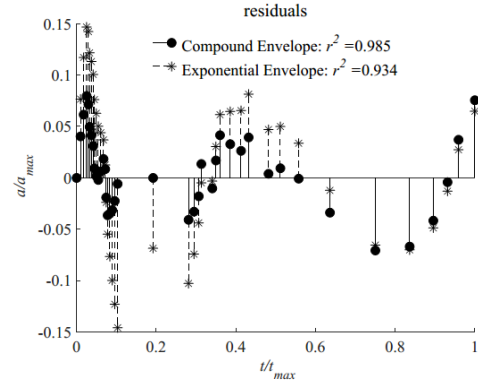


(e)

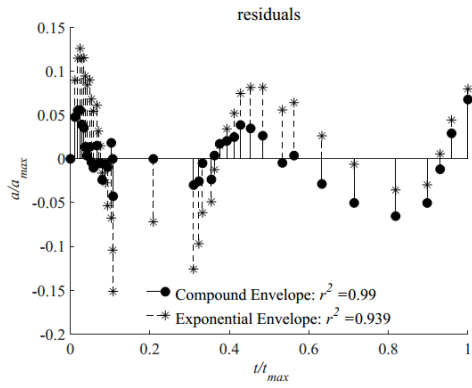
**Figure 9.** Fitted curves of edge envelopes: (a) Group 1; (b) Group 2; (c) Group 3; (d) Group 4; (e) Group 5



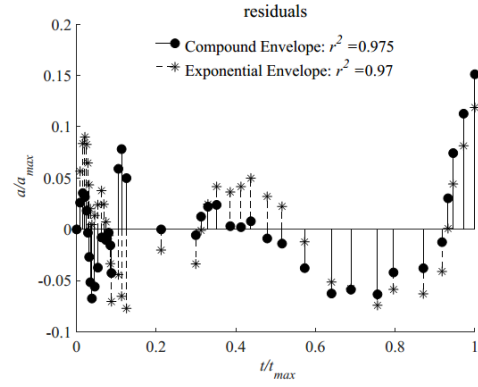
(a)



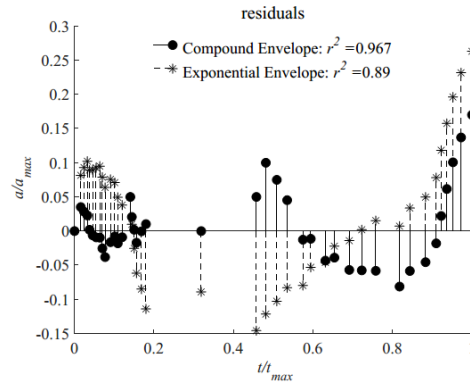
(b)



(c)



(d)



(e)

**Figure 10.** Fitting residuals and  $r^2$  of edge envelopes: (a) Group 1; (b) Group 2; (c) Group 3; (d) Group 4; (e) Group 5

**Table 7** Fitted parameters of exponential envelopes

D5-95	$A$	$\alpha$	$\beta$
5-10	21.530	5.774	6.504
11-15	-49.040	5.481	5.205
16-20	76.243	5.006	5.175
21-30	7.876	3.969	5.576
31-50	-183.029	3.542	3.494

**Table 8** Fitted parameters of compound envelopes

D5-95	$\gamma$	$b_1$	$b_2$
5-10	3.536	0.09	0.21
11-15	3.460	0.11	0.25
16-20	3.766	0.12	0.29
21-30	2.614	0.12	0.28
31-50	3.296	0.19	0.47

#### *Adjust to edge enveloped artificial earthquakes and error analysis*

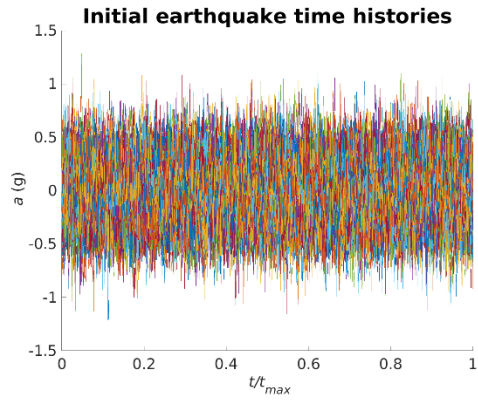
According to Eq.14 to Eq.16, artificial earthquakes' (initial earthquakes) acceleration time histories were generated, and these earthquake based Chinese standard GB50011 response spectrum, and

earthquake intensity is changing from 4.5 to 10, and the increment is 0.5. For each intensity of each D5-95 group, 100 earthquakes were generated. Thus, 1200 earthquakes were generated. Figure11 is acceleration time histories of initial earthquakes. And amplitudes of initial earthquakes are nearly constant values. To make these earthquake signals have the same enhancement and attenuation amplitudes-time changing law as natural earthquakes, these earthquakes are multiplied with compound envelopes and exponential envelopes respectively. Time histories of enveloped earthquakes are shown in Figure12 and Figure13. And to explore effective on earthquake intensity caused by these two types of edge envelopes, mean response spectrums of initial earthquakes and two type edge enveloped earthquakes have been drawn in Figure14. As a result of that some step earthquakes' amplitudes are weakened by envelopes, response spectrums of both compounds enveloped earthquakes and exponential enveloped earthquakes are lower than that of initial earthquakes. And intensities of enveloped earthquakes are decreased compared with initial earthquakes.

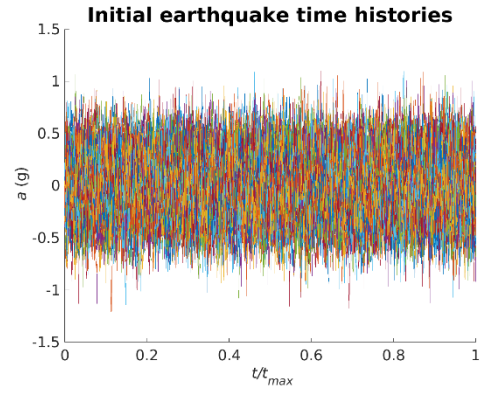
Mean response spectrum's maximum value ratios of initial earthquakes ( $S_{amax(i)}$ ) to exponential enveloped earthquakes ( $S_{amax(e)}$ ) and compound enveloped earthquakes ( $S_{amax(c)}$ ) of each intensity and each D5-95 group is shown in Table 9 and Table 10 respectively. It can be observed that, in each D5-95 group, ratio values of different intensities' earthquakes are similar. And response spectrum calculation of earthquake acceleration time histories is linear, thus mean values of  $S_{amax(i)}/S_{amax(e)}$  and  $S_{amax(i)}/S_{amax(c)}$  of different intensities' earthquakes in each D5-95 group are treated as each D5-95 group's amplitude adjustment coefficient ( $\kappa$ ) for these two envelope type respectively and are shown in Table 11. After enveloped, earthquake time histories are multiplied with the amplitude adjustment coefficient to be adjusted. And the entire process for artificial earthquake acceleration time histories generation is that:

- (1) transferring Chinese standard response spectrum to PSDF as Eq.14,
- (2) generating initial earthquake acceleration time histories  $a(t)_{(in)}$  by the PSDF and Eq.15 and Eq.16,
- (3) enveloping and adjusting  $a(t)_{(in)}$  by Eq.20 and get final signals  $a(t)$ .

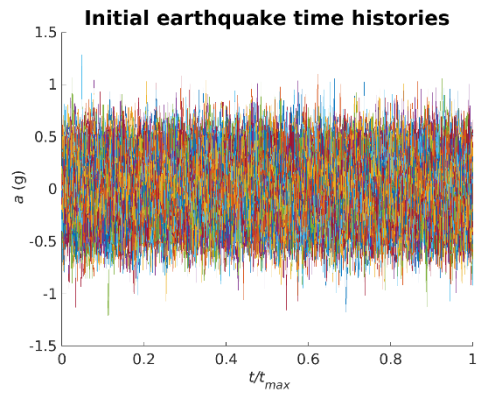
$$a(t) = \kappa \cdot I(t) \cdot a(t)_{(in)} \quad (20)$$



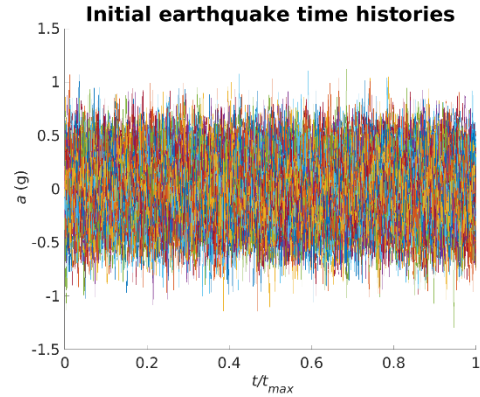
(a)



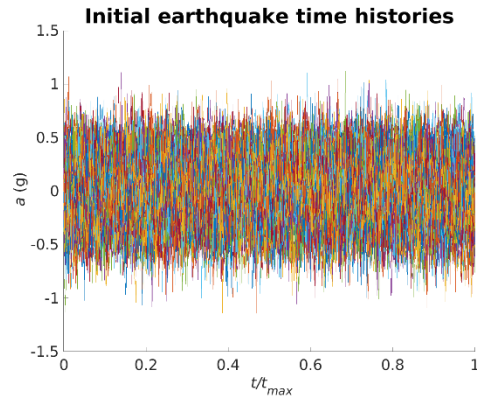
(b)



(c)

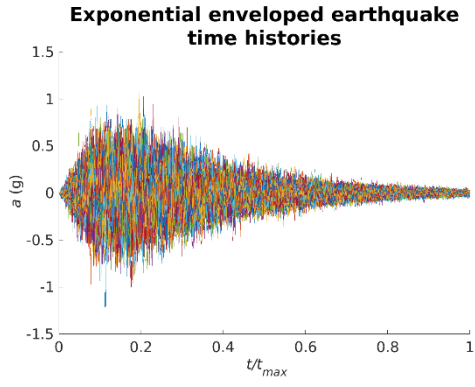


(d)

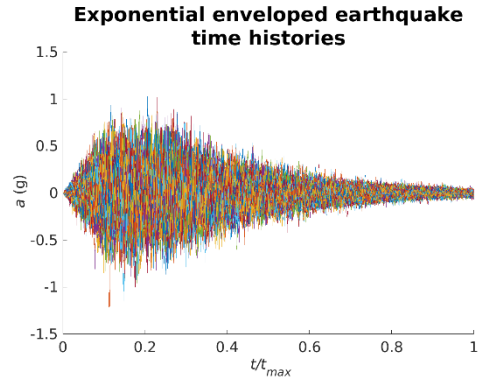


(e)

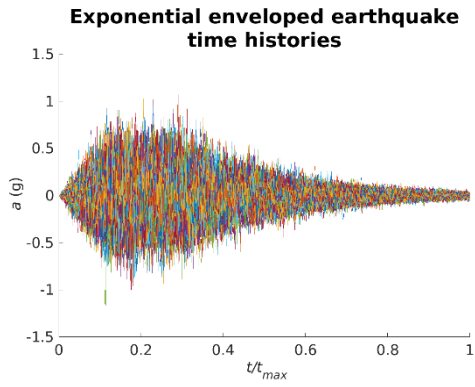
**Figure 11.** Acceleration time histories of initial earthquakes: (a) Group 1; (b) Group 2; (c) Group 3; (d) Group 4; (e) Group 5



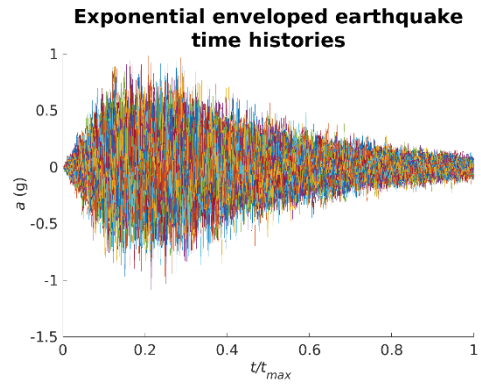
(a)



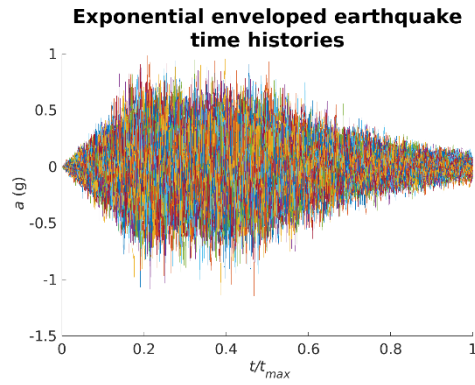
(b)



(c)

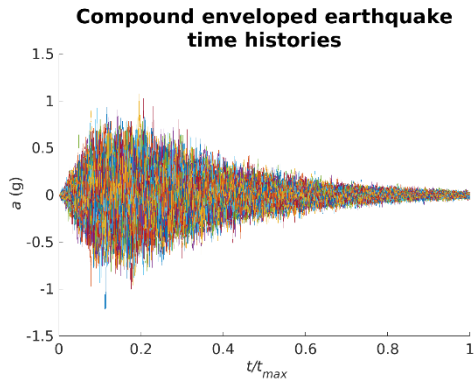


(d)

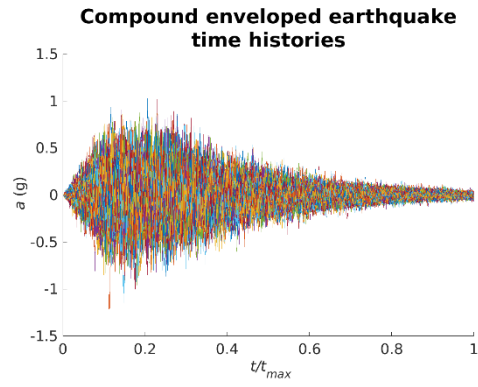


(e)

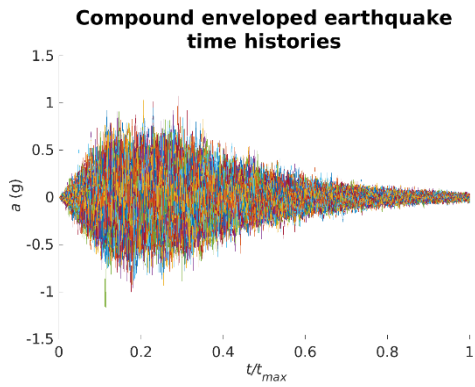
**Figure 12.** Acceleration time histories of exponential enveloped earthquakes: (a) Group 1; (b) Group 2; (c) Group 3; (d) Group 4; (e) Group 5



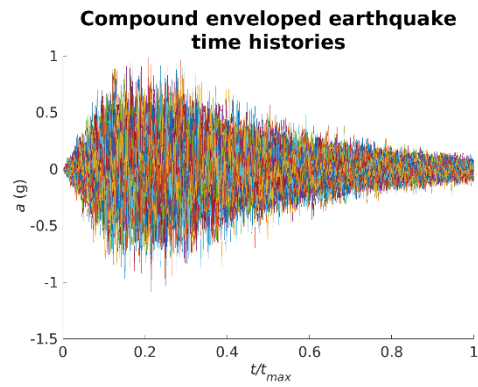
(a)



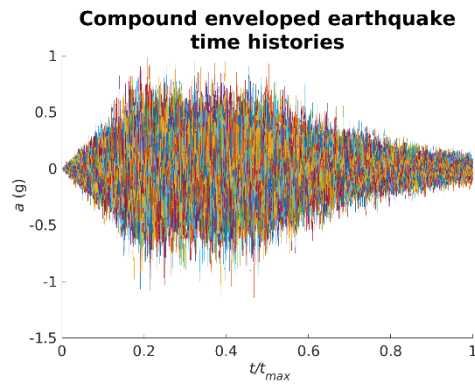
(b)



(c)



(d)



(e)

**Figure 13.** Acceleration time of compound enveloped earthquakes: (a) Group 1; (b) Group 2; (c) Group 3; (d) Group 4; (e) Group 5

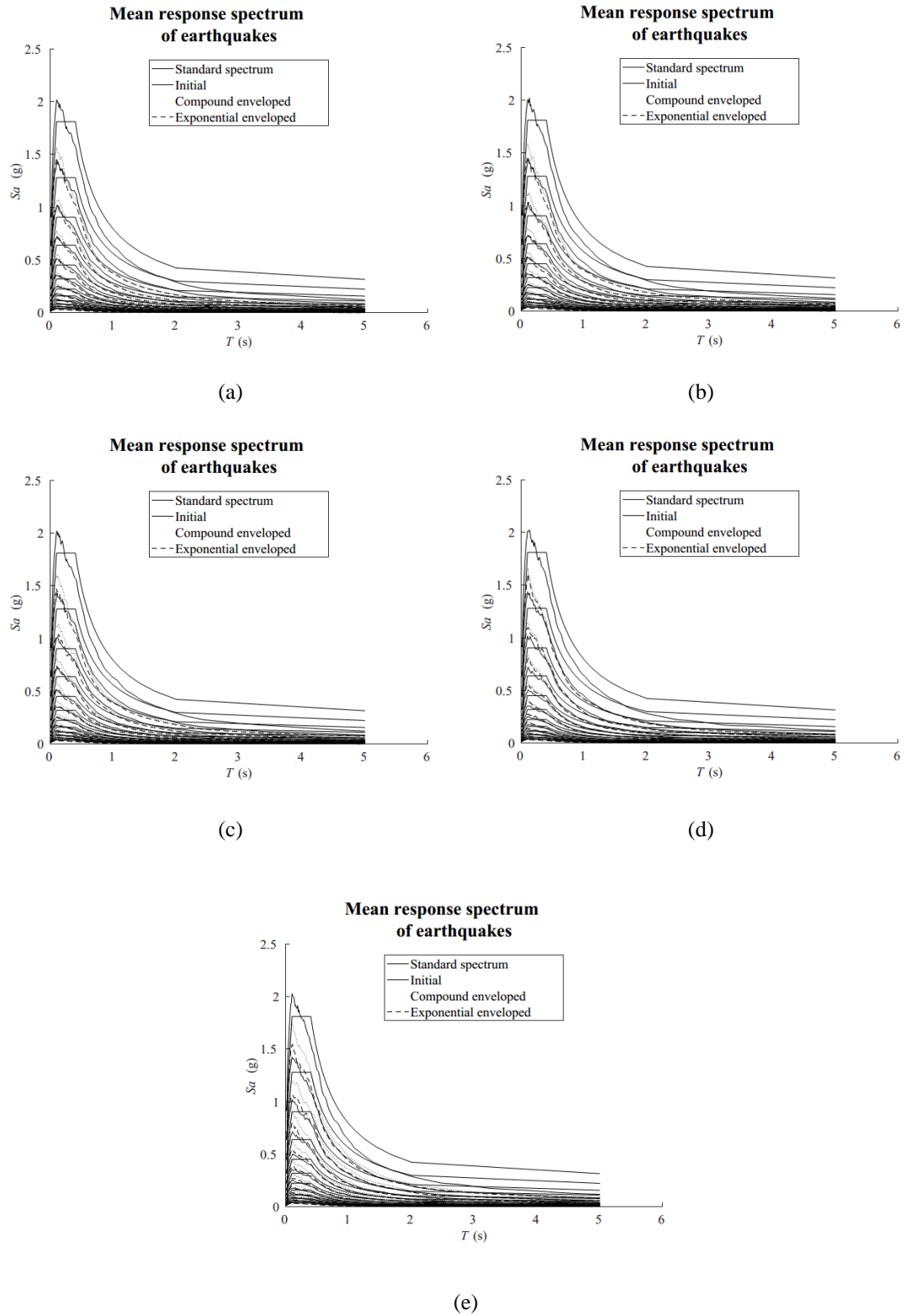


**Figure 14.** Mean response spectrums of earthquakes: (a) Group 1; (b) Group 2; (c) Group 3; (d) Group 4; (e) Group 5

**Table 9**  $S_{amax(i)}/S_{amax(e)}$ 

Intensity	D5-95				
	5-10	11-15	16-20	21-30	31-50
4.5	1.380	1.324	1.377	1.278	1.313
5	1.385	1.389	1.358	1.293	1.307
5.5	1.399	1.339	1.376	1.265	1.287
6	1.401	1.360	1.387	1.280	1.311
6.5	1.408	1.363	1.366	1.273	1.310
7	1.427	1.367	1.357	1.295	1.298
7.5	1.416	1.370	1.359	1.320	1.302
8	1.389	1.409	1.389	1.253	1.333
8.5	1.394	1.383	1.360	1.279	1.320
9	1.359	1.397	1.388	1.254	1.305
9.5	1.395	1.389	1.352	1.317	1.281
10	1.384	1.391	1.368	1.278	1.304

**Table 10**  $S_{amax(i)}/S_{amax(c)}$ 

Intensity	D5-95				
	5-10	11-15	16-20	21-30	31-50
4.5	1.291	1.214	1.259	1.226	1.153
5	1.296	1.275	1.239	1.258	1.160
5.5	1.325	1.232	1.256	1.221	1.130
6	1.325	1.251	1.265	1.235	1.152
6.5	1.312	1.256	1.246	1.228	1.158
7	1.336	1.270	1.245	1.261	1.147
7.5	1.326	1.262	1.241	1.268	1.153



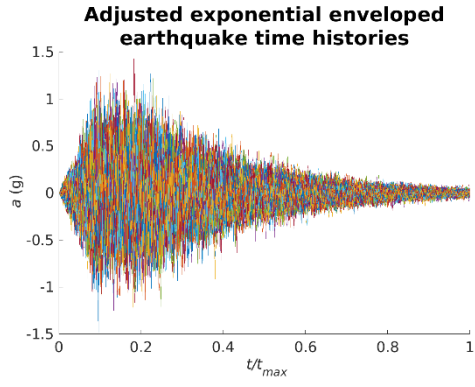
**Continue-table 10**  $S_{amax(i)}/S_{amax(c)}$ 

Intensity	D5-95				
	5-10	11-15	16-20	21-30	31-50
8	1.304	1.286	1.265	1.213	1.171
8.5	1.305	1.275	1.237	1.242	1.157
9	1.274	1.284	1.266	1.215	1.152
9.5	1.300	1.278	1.238	1.271	1.136
10	1.288	1.287	1.256	1.231	1.140

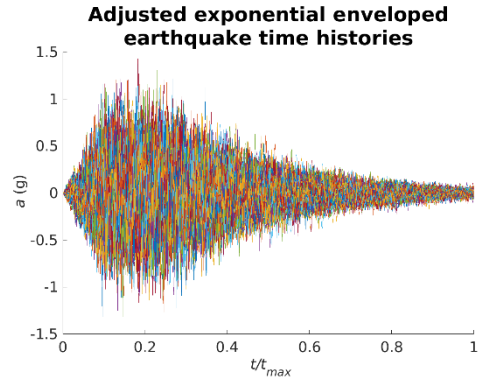
**Table 11** Amplitude adjustment coefficients ( $\kappa$ ) of enveloped earthquakes

D5-95	$\kappa$	
	compound envelope	Exponential envelope
5-10	1.307	1.395
11-15	1.264	1.373
16-20	1.251	1.370
21-30	1.239	1.282
31-50	1.151	1.306

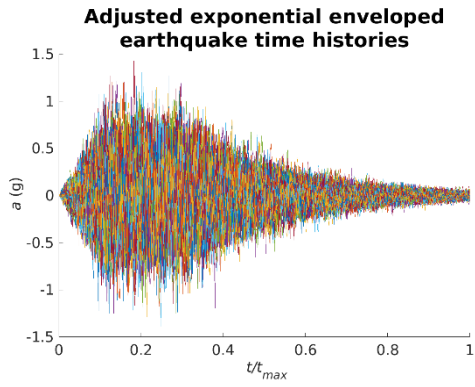
Acceleration time histories of adjusted earthquakes from those initial earthquakes are shown in Figure15 and Figure16. And Figure17 is the mean response spectrums of adjusted earthquakes. It can be observed that earthquakes' response spectrum shapes of earthquakes are not changed significantly before and after adjusted, and spectrums' max values of adjusted earthquakes are similar to of initial earthquakes. Table 12 and Table 13 are  $r^2$  for the fitting by these two types' adjusted enveloped earthquakes' mean spectrums to initial earthquakes' mean spectrums respectively. All values  $r^2$  are larger than 0.9. It reflects that after enveloped and multiplied with adjustment coefficient, the mean responses of earthquakes are 90% explaining the accuracy to of initial earthquakes which are according to standard GB50011 designed responses.



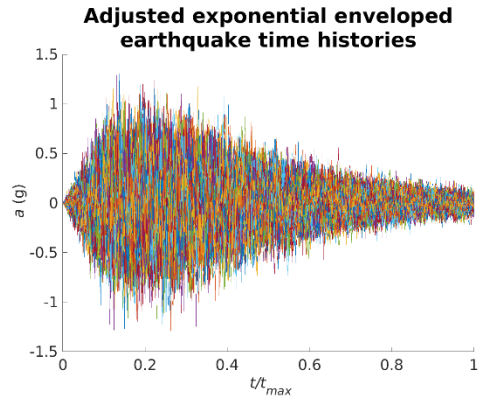
(a)



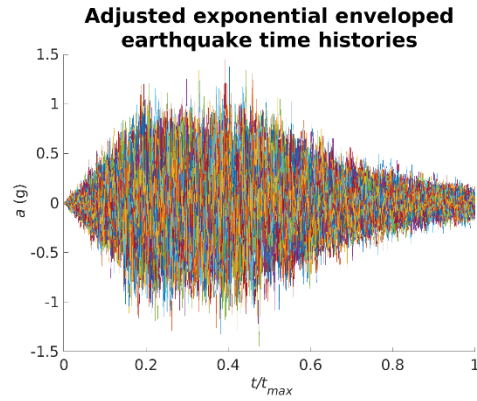
(b)



(c)

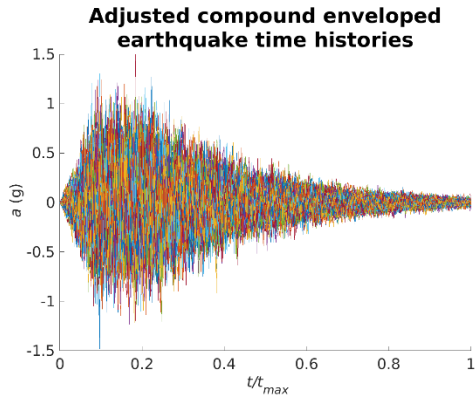


(d)

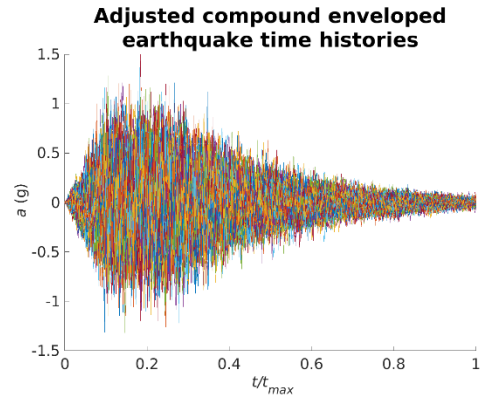


(e)

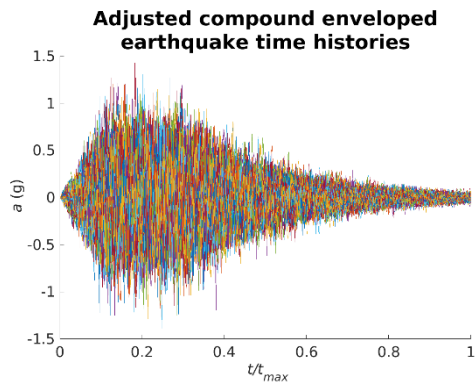
**Figure 15.** Acceleration time histories of adjusted exponential enveloped earthquakes: (a) Group 1; (b) Group 2; (c) Group 3; (d) Group 4; (e) Group 5



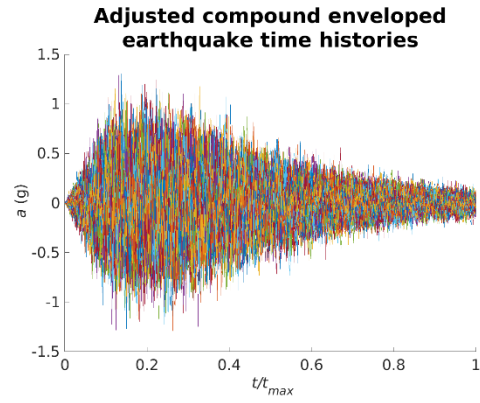
(a)



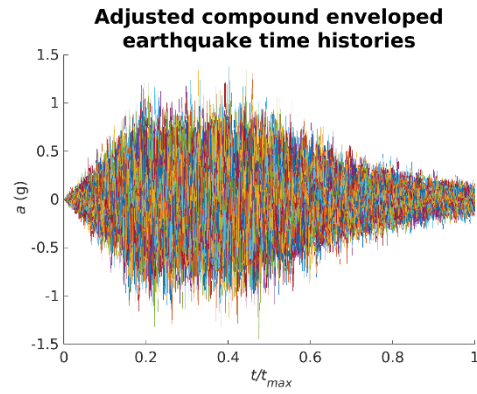
(b)



(c)



(d)



(e)

**Figure 16.** Acceleration time histories of adjusted compound enveloped earthquakes: (a) Group 1; (b) Group 2; (c) Group 3; (d) Group 4; (e) Group 5

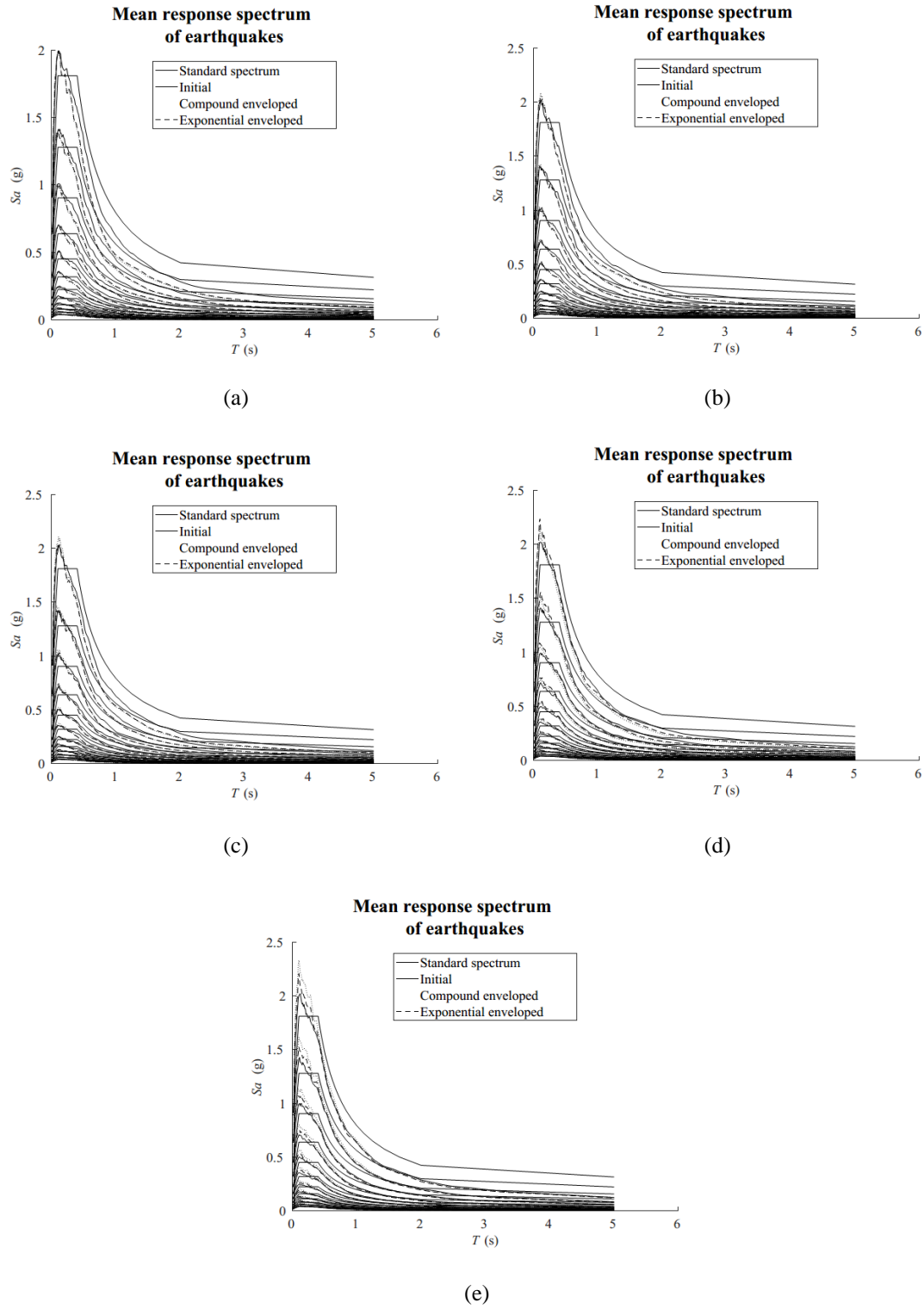


**Figure 17.** Mean response spectra of adjusted earthquakes: (a) Group 1; (b) Group 2; (c) Group 3; (d) Group 4; (e) Group 5

**Table 12** Mean spectrums'  $r^2$  between adjusted exponential enveloped earthquakes and initial earthquakes

Intensity	D5-95				
	5-10	11-15	16-20	21-30	31-50
4.5	0.978	0.982	0.986	0.989	0.994
5	0.985	0.989	0.989	0.990	0.994
5.5	0.981	0.984	0.985	0.988	0.994
6	0.982	0.986	0.988	0.989	0.995
6.5	0.980	0.981	0.988	0.990	0.995
7	0.980	0.985	0.984	0.985	0.995
7.5	0.987	0.991	0.982	0.985	0.995
8	0.984	0.989	0.985	0.986	0.995
8.5	0.980	0.982	0.991	0.992	0.997
9	0.979	0.984	0.988	0.989	0.994
9.5	0.983	0.985	0.988	0.991	0.996
10	0.981	0.982	0.985	0.987	0.995

**Table 13** Mean spectrums'  $r^2$  between adjusted compound enveloped earthquakes and initial earthquakes

Intensity	D5-95				
	5-10	11-15	16-20	21-30	31-50
4.5	0.973	0.977	0.980	0.987	0.991
5	0.980	0.984	0.985	0.987	0.991
5.5	0.976	0.978	0.979	0.985	0.991
6	0.978	0.982	0.983	0.986	0.992
6.5	0.974	0.974	0.983	0.987	0.991
7	0.976	0.979	0.979	0.981	0.992
7.5	0.984	0.986	0.976	0.982	0.992
8	0.979	0.984	0.980	0.983	0.992
8.5	0.976	0.976	0.987	0.990	0.994
9	0.974	0.978	0.983	0.986	0.990
9.5	0.979	0.980	0.982	0.988	0.994
10	0.977	0.976	0.979	0.984	0.991

## Conclusion

According to normalized natural earthquakes statistics, edge envelope curves can be drawn and the coverage rate was proposed to describe the percentage of earthquake peak point samples which are covered by the edge envelope. Under the 75% coverage rate, edge envelopes of different D5-95 groups were fitted as exponential envelope function and compound envelope function, and parameters were fitted. Comparing initial earthquakes and enveloped earthquakes, amplitude adjustment coefficients were proposed. And by using function parameters and amplitude adjustment coefficients,  $r^2$  of adjusted enveloped earthquakes' mean spectrums to initial earthquakes' mean spectrums are more than 0.9. It reflects that after enveloped and multiplied with adjustment coefficient mean responses of earthquakes are similar to initial earthquakes which are according to standard GB50011 designed responses. And this opening method can generate earthquakes with different statistical accuracies and different spectrum forms according to research needs by adjusting coverage rate and earthquake samples.

## Acknowledgments

Natural earthquake data were downloaded from PEER Strong Ground Motion Databases (<https://peer.berkeley.edu/peer-strong-ground-motion-databases>). And the calculation is supported by Institute for Risk and Reliability, University Hannover.

## Reference

- [1] Malhotra, P. K. (2011). Seismic response spectra for probabilistic analysis of nonlinear systems. *Journal of structural engineering*, 137(11), 1272-1281. [https://doi.org/10.1061/\(ASCE\)ST.1943-541X.0000373](https://doi.org/10.1061/(ASCE)ST.1943-541X.0000373)
- [2] Feldgun, V.R., Karinski, Y.S., Yankelevsky, D.Z., Kochetkov, A.V. (2016). A new analytical approach to reconstruct the acceleration time history at the bedrock base from the free surface signal records. *Soil Dynamics & Earthquake Engineering*, 85, 19-30.
- [3] GB50011. (2010). *Code for Building Seismic Desgin*. Ministry of housing and urban rural development of the people's Republic of China.
- [4] GB50068. (2018). *Unified Standard for Reliability Design of Building Structures*. Ministry of housing and urban rural development of the people's Republic of China.
- [5] Zio, E. (2013). *The Monte Carlo Simulation Method for System Reliability and Risk Analysis*. Springer.
- [6] GB/T17742. (2008). *The Chinese Seismic Intensity scale*. General Administration of quality supervision, inspection and Quarantine of the people's Republic of China.
- [7] Shin, G., Song, O. (2016). A Time-Domain Method to Generate Artificial Time History from a Given Reference Response Spectrum. *Nuclear Engineering and Technology*, 48, 831-839.
- [8] Kost, G., Tellkamp, T., Kamil, H., Gantayat, A., Weber, F. (1978). Automated generation of spectrum-compatible artificial time histories. *Nuclear Engineering & Design*, 45(1), 243-249.

- [9] EC8: EN1998-1. (2004). *Design of structures for earthquake resistance*. EUROPEAN COMMITTEE FOR STANDARDIZATION.
- [10] ASCE/SEI 7-16. (2016). *Minimum Design Loads and Associated Criteria for Buildings and Other Structures*. AMERICAN SOCIETY OF CIVIL ENGINEERING.
- [11] Kaul, M. K. (1978). Stochastic characterization of earthquakes through their response spectrum. *Earthquake Engineering & Structural Dynamics*, 6(5), 497-509.
- [12] Salmon, M. W., & Kuilanoff, G. (1991). *Generation of artificial earthquake time histories for seismic design at Hanford*, Washington (No. CONF-9110122--).
- [13] Kung, S. Y., & Pecknold, D. A. (1982). *Effect of ground motion characteristics on the seismic response of torsionally coupled elastic systems*. University of Illinois Engineering Experiment Station. College of Engineering, University of Illinois at Urbana-Champaign.
- [14] Jennings, P. C., Housner, G. W. and Tsai, N. C. (1968). *Simulated Earthquake Motions*, Report, Earthquake Engineering Research Laboratory, California Institute of Technology.  
[https://authors.library.caltech.edu/26504/1/Jennings\\_1968.pdf](https://authors.library.caltech.edu/26504/1/Jennings_1968.pdf)
- [16] Trifunac, M. D., & Brady, A. G. (1975). A study on the duration of strong earthquake ground motion. *Bulletin of the Seismological Society of America*, 65(3), 581-626.
- [17] Ritter, A., & Muñoz-Carpena, R. (2013). Performance evaluation of hydrological models: Statistical significance for reducing subjectivity in goodness-of-fit assessments. *Journal of Hydrology*, 480, 33-45.